Supporting Information

Ultrasensitive surface-enhanced Raman scattering sensing of Cr(VI) with Au@Ag nano-sea urchins paper-tip substrate

Ronghui Xu [a], Lu Tan [a], Wei Xu [b], Li Xiao [a], Yingping Zheng [, a, b], Ying Li [*, a] and Yongbing Lou [*, a]*

[a] School of Chemistry and Chemical Engineering, Southeast University, Nanjing, 211189, P. R. China.

[b] Analysis and Testing Center, Southeast University, Nanjing 211189, P. R. China.

***Email(s):** seuzheng@seu.edu.cn (Prof. Yingping Zheng); yingli@seu.edu.cn (Assoc. Prof. Ying Li); lou@seu.edu.cn (Prof. Yongbing Lou).

Table of Contents

Materials and Apparatus

Materials. Chloroauric acid trihydrate ($HAuCl_4 \cdot 3H_2O$, 99%), sodium lauryl sulfate ($C_{12}H_{25}SO_4Na$, 99%), potassium dichromate ($K_2Cr_2O_7$, 99%), polyethylene pyrrolidone ((C_6H_9NO) n) were purchased from Macklin Biochemical Technology Co., Ltd. (Shanghai, China). Silver nitrate ($AgNO_3$, 99%), ascorbic acid (AA, 99%), ethanol (C_2H_5OH, 99%), crystal violet (CV, 99%), acetone (CH_3COCH_3, 99%), sulfuric acid (H_2SO_4, 96%), hydrochloric acid (HCl, 38%), sodium citrate dihydrate ($Na_3C_6H_5O_7 \cdot 2H_2O$, 99%) were bought from Sinopharm Chemical Reagent Co., Ltd. (Shanghai, China). 2-mercapto-1-methylimidazole ($C_4H_6N_2S$, 98%) was obtained from J&K Scientific Co., Ltd. (Beijing, China). Ammonia (NH_4OH, 28%) and hydrogen peroxide (H_2O_2, 30%) were acquired from Shanghai Lingfeng Chemical Reagent Co., Ltd. (Shanghai, China). Filter paper (New Star Brand) was purchased from Hangzhou Special Paper Industry Co., Ltd. (China). Milli-Q water (resistivity of 18.2 $M\Omega \cdot cm^{-1}$) was utilized to prepare all reagents.

Apparatus. High-resolution transmission electron microscopy (HRTEM) images were collected by a Talos F200X TEM (Thermo Fisher, USA). Ultraviolet-visible (UV-vis,) spectra analysis was carried out with a 2600 UV-vis spectrophotometer (Shimadzu, Japan). The scanning electron microscopy (SEM) images collected by an Ultra Plus Field emission scanning electron microscope (Zeiss, Germany). The Xplora Plus Raman Microscopy (HORIBA, Japan) was used to detect the Raman spectrum of analytes. The excitation laser used for CV as a Raman reporter molecule has a wavelength of 638 nm and a power of 5 mW. The process of analyzing Cr(VI) used a

laser wavelength of 785 nm and a power of 10 mW. The integration time for each spectrum was set to 10 s.

Preparation of Au NSUs

An improved seed growth method was employed to synthesize Au NSUs.[1] The specific steps were as follows: Firstly, Au seeds were synthesized by rapidly adding 7.5 mL of aqueous trisodium citrate (1 wt%) to 50 mL of 1 mM $HAuCl_4$ solution, stirring vigorously at 100 °C for 15 min, and then cooling naturally to room temperature. Prior to the subsequent synthesis step, the produced Au seed was filtered through a 0.22 μm microporous membrane.

Secondly, Au NSUs was synthesized by adding 1 mL of filtered Au seed into a round-bottomed flask containing 100 μL HCl (1 M) and 100 mL $HAuCl_4$ (0.25 mM) under vigorous stirring. Subsequently, 500 μL ascorbic acid (100 mM) and 2 mL of $AgNO_3$ (0.75 mM) was concurrently added into the mixture. With the reaction proceeding, the color of the reaction solution changed from light red to blue-black. After 1 min, 10 mL of polyvinylpyrrolidone (PVP) solution was added.[2] As a dispersant, PVP prevented the accumulation of nanoparticles through the repulsion generated by its hydrophobic carbon chains and interactions (steric hindrance effect). The generated Au NSUs was then centrifuged at 8000 rpm for 15 min and dispersed in 100 mL of deionized water.

Preparation of Au@Ag NSUs

Au@Ag NSUs were acquired by adding 50 μL $AgNO_3$ (100 mM), 25 μL ascorbic acid (100 mM) and 25 μL NH_4OH (14.84 M) in sequence to 25 mL Au NSUs solution under stirring at 700 rpm at 25 °C.[3] The color of solution quickly changed from blue-black to reddish-brown. Then, 1 mL of 0.01M sodium dodecyl sulfate (SDS) was added as a surfactant to disperse the particles.[4] An amphiphilic SDS has good dispersion ability, in which the alkane tail is oleophilic and sulfate tail is hydrophilic. The suspension was centrifuged at 8000 rpm for 15 min and dispersed in 2.5 mL deionized water.

Fabrication of paper-tip SERS substrate

Firstly, the filter paper was cut to 10-degree angle and the length of paper tip was 50 mm. Then the paper tip was placed on the iron stand, and the temperature of the heating plate was set at 70 ℃. 20 μL Au@Ag NSUs droplet was continuously dripped at the 16 mm distance from the paper-tip. The next droplet was dropped after the previous one had dried, and this process was repeated for five times.

SERS detection of Cr(VI) in standard solution and SERS analysis

A series of Cr(VI) standard solutions at varying concentrations were prepared. For Cr(VI) detection, 90 μL Au@Ag NSUs and 20 μL methimazole solution were firstly mixed for 30 min, followed by 100 μL Cr(VI) solution. Then, 20 μL NaCl solution was added to the mixture to help the nanoparticles agglomerate, creating more localized hot spots and thereby enhancing the strength of the Raman signal. 20 μL mixture was drawn with a pipette gun and dripped at the 16 mm distance from the paper-tip. The next droplet was dropped after the previous one had dried, and this process was repeated for five times. When the sample was dried, the paper tip was taken down and Raman spectra were collected at the paper tip. The SERS signals of three detection positions within 1-mm distance from the paper-tip end were measured randomly and the average value was obtained to represent the SERS signal of the paper tip.

Detection of real water samples

The real water samples were acquired from the JiuLong Lake in campus and tap water. The samples of tap water and lake water were spiked with varying concentrations of Cr(VI) after being filtered through a 0.22 μm membrane to remove particulates.

Calculations of enhancement factor

The SERS activity of the Au@Ag NSUs was evaluated by using CV as the probing molecule because of its well-established vibrational features. The measurements are performed on isolated silicon slices. When Au@Ag NSUs were used as the substrate, the characteristic vibrations observed at 439, 559, 605, 723, 758, 914, 978, 1172, 1298, 1379, 1418, 1447, 1478, 1534, 1585, 1618 cm^{-1}, can be clearly identified and attributed. The limit of detection is around 10^{-10} M. The SERS performance has been studied

quantitatively by calculating the SERS enhancement factor (EF), which can be determined by the following equation:

$$EF = I_{SERS}C_0/I_0C_{SERS} \quad (1)$$

Where I_{SERS} and C_{SERS} are the SERS intensity and the concentrations of CV under the SERS experiment, respectively. I_0 and C_0 are the SERS intensity and the concentration of CV under normal SERS measurement with CV solution on a bare silicon substrate, respectively. The EF calculated is about 2.71×10^7 with $C_0 = 10^{-3}$ M, $C_{SERS} = 10^{-11}$ M, I_{SERS} (1618 cm^{-1}) = 157.46, and I_0 (1618 cm^{-1}) =580.34, suggesting great performance of the obtained Au@Ag NSUs.

The calculation of limit of detection (LOD)

According to the formula LOD = 3σ/S, where σ and S represent the standard deviation of the blank samples and the slope of the line (at least 3 times), respectively.

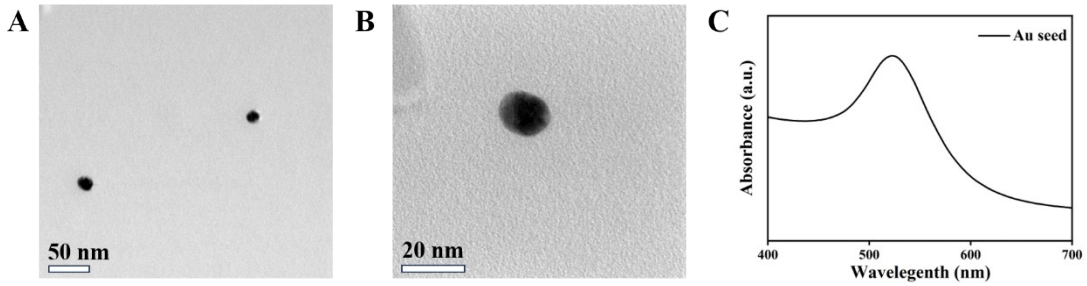

Fig. S1. (A) (B) TEM images of Au seed and (C) UV-vis spectrum of Au seed.

Au NSUs with different lengths and branch numbers, named Au NSU-1, Au NSU-2, and Au NSU-3, were synthesized by 0.5, 0.75, and 1 mM $AgNO_3$, respectively. TEM images indicated that Au NSU-1 was still mainly rough and spherical with a few branching, while Au NSU-2 and Au NSU-3 exhibited more branches (Fig. S3). UV-vis spectra revealed a significantly red-shifted LSPR band with the concentration of $AgNO_3$ increased (Fig. S3A). This was primarily due to the increase in the length and number of branches of Au NSUs.[5] Au NSUs-2 generated higher enhancement than Au NSUs-1 and Au NSUs-3 clearly (Fig. S3B and Fig. S3C). Therefore, Au NSUs-2 was chosen for subsequent Ag coating. Similarly, the thickness of the silver shell was regulated by changing the volume of the precursor. As the volume of the precursor gradually increased from 30 μL to 60 μL, the UV-vis absorption spectra revealed Au@Ag NSUs gradually showed a wide and blue-shifted LSPR band (Fig. S3D). TEM images indicated that the multiple long branches of the bimetal Au@Ag NSUs decreased as well as the overall trend was more spherical as precursor increased (Fig. S4). The phenomenon was in agreement with the findings proposed by Tuan Vo-Dinh et al.[6] The outcropping part of the branches decreased or even was completely buried under the increasing silver shell when $AgNO_3$ continued to increase. As illustrated in Fig. S3E and Fig. S3F, the Raman intensity of CV reached its maximum value with 50 μL $AgNO_3$. Nevertheless, the signal intensity was slightly weakened when the volume increased continuously, because transmission of CV signals was hampered by thicker Ag shells.

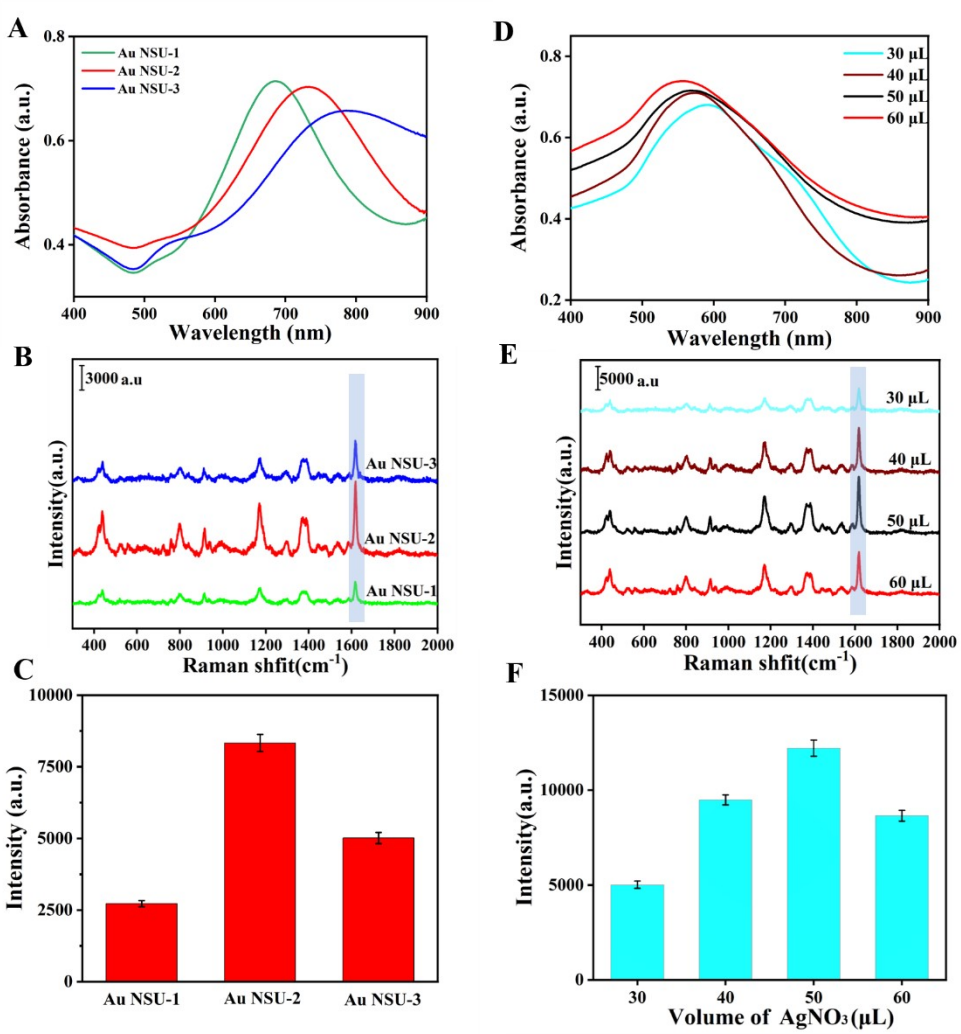

Fig. S2. (A) UV-vis spectra of Au NSUs. (B) Raman spectra of CV (1×10^{-4} M) on different Au NSUs. (C) Comparison of peak intensity of CV at 1618 cm^{-1} on different Au NSUs. (D) UV-vis spectra of different Au@Ag NSUs. (E) Raman spectrum of CV (1×10^{-6} M) on different Au@Ag NSUs. (F) Comparison of peak intensity of CV at 1618 cm^{-1} on different Au@Ag NSUs.

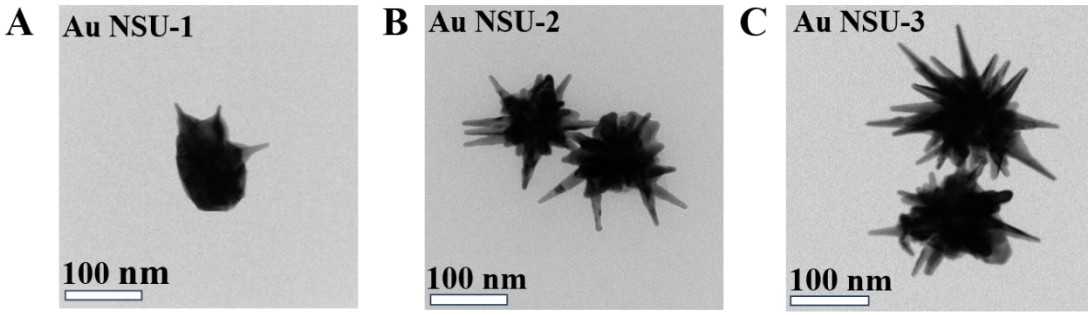

Fig. S3. TEM images of (A) Au NSU-1, (B) Au NSU-2 and (C) Au NSU-3.

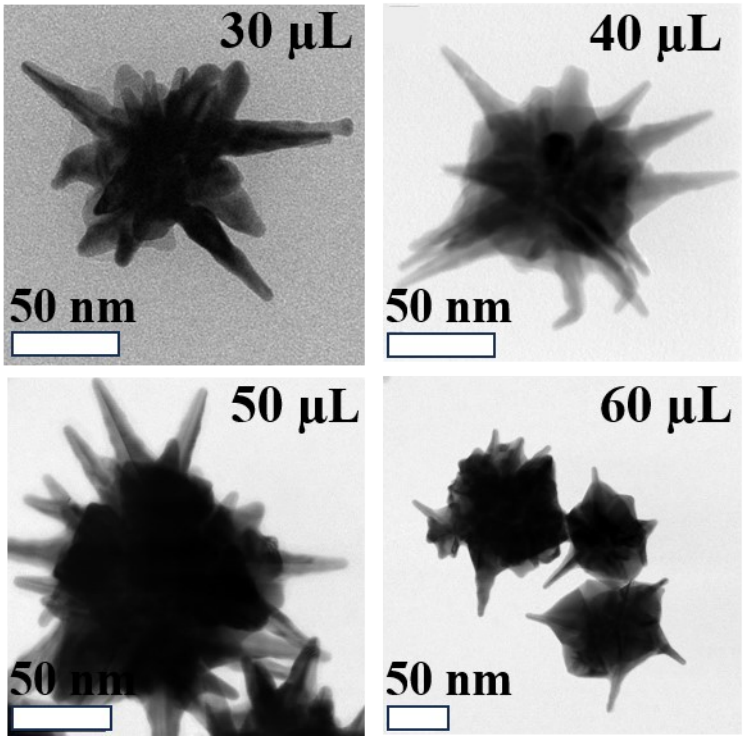

Fig. S4. TEM images of Au@Ag NSUs when 100 mM $AgNO_3$ volume was 30 µL, 40 µL, 50 µL and 60 µL.

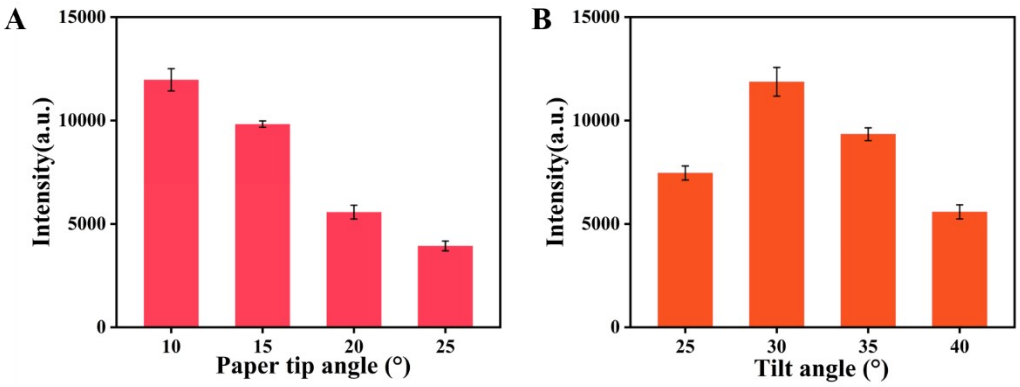

Fig. S5. (A) Raman signal intensities of CV at 1618 cm^{-1} at the paper-tip SERS substrate from different paper-tip angles. (B) Influence of inclination angle of the paper tip on SERS signal intensity. The SERS excitation laser: 638 nm.

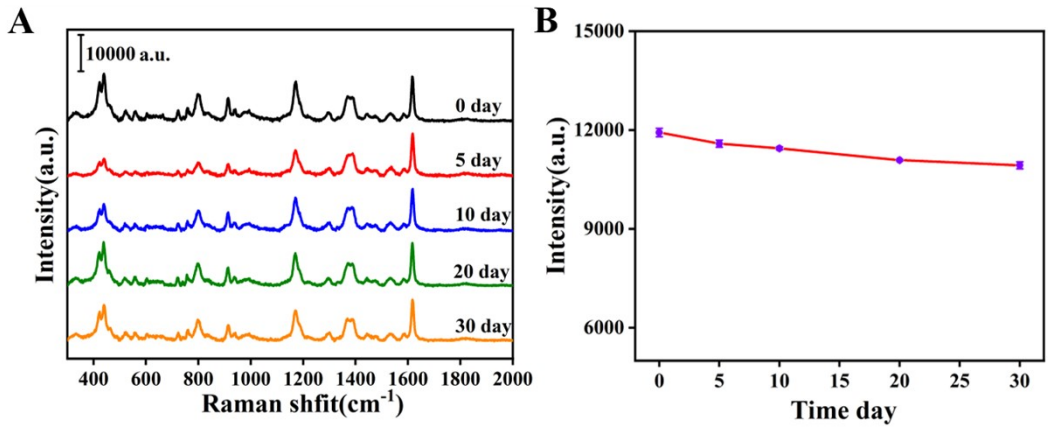

Fig. S6. (A) Raman spectrum of Au@Ag NSUs with CV after storing at 4 °C temperature for 0, 5, 10, 20 and 30 d. (B) Plots of the 1618 cm^{-1} peak intensity of Au@Ag NSUs with CV under different storage time. The SERS excitation laser: 638 nm.

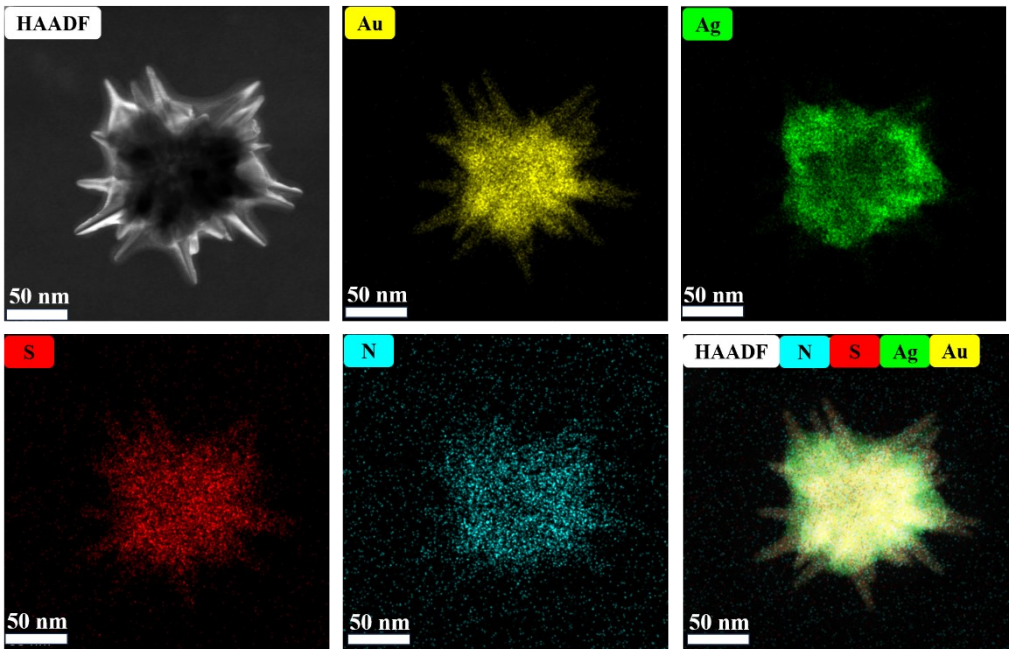

Fig. S7. Elemental mapping images of Au@Ag NSUs functionalized with methimazole.

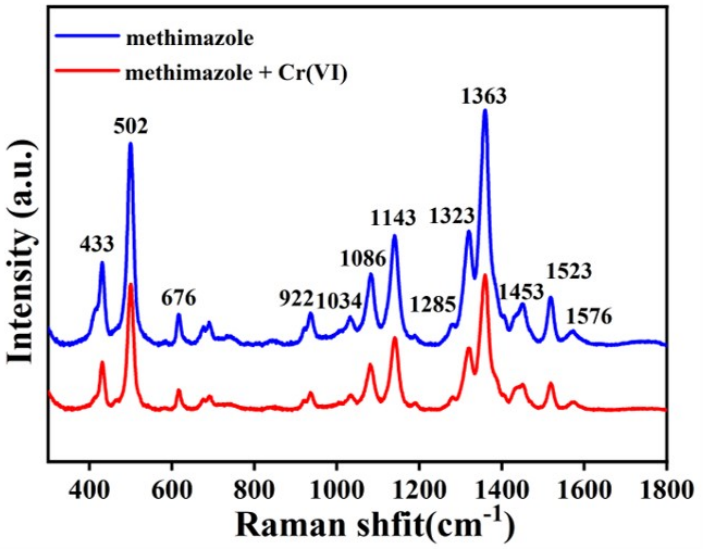

Fig. S8. Comparison of Raman spectra before and after the oxidation-reduction reaction between methimazole and Cr(VI). The SERS excitation laser: 785 nm.

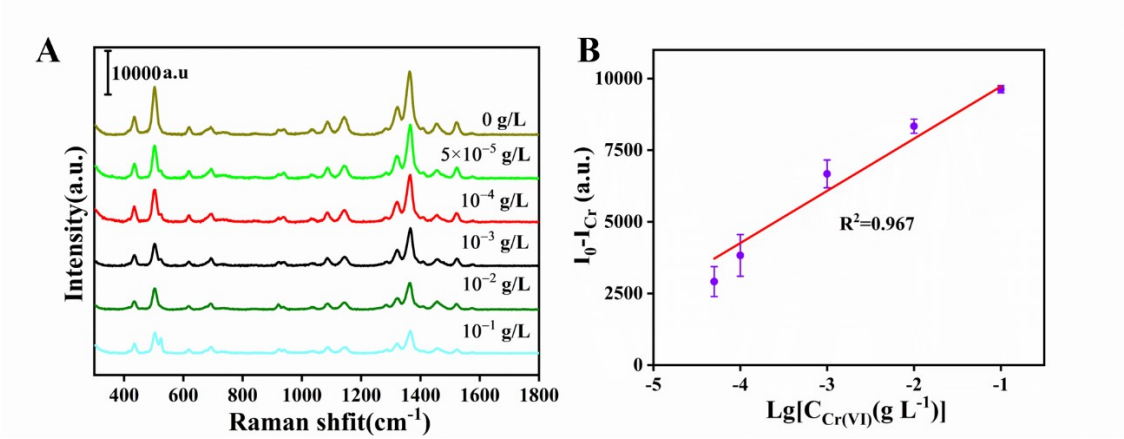

Fig. S9. (A) Raman spectrum of methimazole with Cr(VI) at different concentrations when Au@Ag NSUs were replaced with Au NSUs. (B) Calibration curve for Cr(VI).

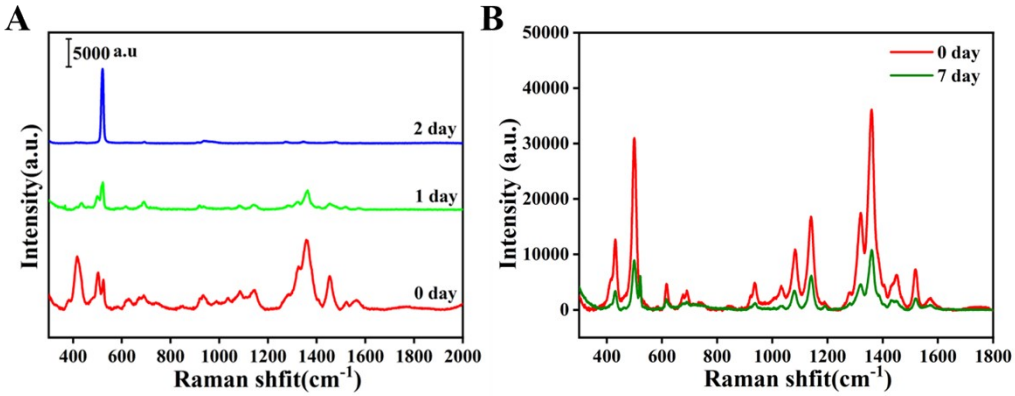

Fig. S10. (A) Raman spectrum of methimazole on the unfunctionalized Au@Ag NSUs paper-tip substrate exposed to air for 0, 1 and 2 d. (B) Raman spectrum of the methimazole functionalized

with Au@Ag NSUs on paper-tip substrate exposed to air for 0 and 7 d. The SERS excitation laser: 785 nm.

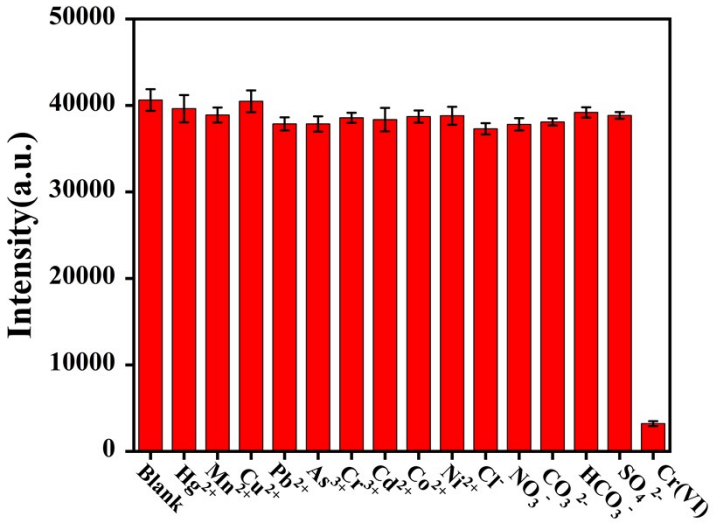

Fig. S11. Specificity of Cr(VI) detection by SERS. The SERS excitation laser: 785 nm.

Table S1. Raman band assignments of CV.[7]

Raman shift (cm^{-1})	Band assignment
439	$\delta_s(CNC)/\delta_{as}(CCC)_{ring}$
559	$\gamma(CCC)/\delta(CNC)/\delta(CC_{center}C)$
605	$\delta(CCC)/\delta(CNC)/\nu_s(CC_{center}C)$
723	$\delta(CCC)_{breathing}$
758	$\nu_s(CC_{center}C)/\nu(CN)/\gamma(CCC)_{ring}$
914	$\delta(CC_{center}C)/\delta(CCC)_{breathing}$
978	$\delta(CCC)_{breathing}$
1172	$\nu_{as}(CC_{center}C)/\delta(CCC)_{breathing}$
1298	$\nu(CN)/\nu_{as}(CCC)_{ring}$
1379	$\nu_{as}(CC_{center}C)/\delta(CH3)/\nu(CN)$
1418	$\delta(CH)/\delta_s(CH3)/\delta(CCC)_{ring}/\nu(CN)$
1447	$\nu_{as}(CCC)_{ring}/\delta_s(CH3)$
1478	$\delta_{as}(CH3)$
1534	$\delta_s(CH3)$
1585	$\nu_{as}(CCC)_{ring}$
1618	$\nu_s(CCC)_{ring}/\nu_s(CC_{center}C)$

Table S2. Raman band assignments for peak obtained during Cr(VI) detection.[8]

Raman shift (cm^{-1})	Band assignment
433	Ring rotation, C-N-S bend
502	C-N-S bend
676	Ring bending, ring CH(NH) bend
922	Ring bending, ring CH(NH) bending, C-N-S bend
1034	In-plane ring bending
1086	Ring CN stretching, ring CH(NH)
1143	C-N stretching
1285	Ring breathing, C-N stretching, ring CH(NH) bending
1323	C-N stretching, ring bending, ring CH(NH) bending
1363	C-N stretching, ring bending, ring CH(NH) bending
1453	C-S stretching, ring CN stretching, NH bend
1523	C-C stretching
1576	C-C stretching, ring CH(NH) bend

Table S3. Comparison of various reported methods for Cr(VI) analysis.

Methods	LOD	Reference
Electrochemistry	0.046 μM	[9]
Electrochemistry	0.16 μM	[10]
Fluorescence	20 nM	[11]
Fluorescence	23 nM	[12]
Colorimetry	0.52 μM	[13]
Colorimetry	0.04 μM	[14]
Atomic absorption spectrometry	15 nM	[15]
SERS (Fe_3O_4-Au@TiO_2)	0.05 μM	[16]
SERS (Fe_3O_4/m-ZrO_2/Ag)	0.05 μM	[17]
SERS (Au@Ag NSUs)	18.4 pM	This work

Table S4. Analytical results of practical water samples.

Spiked Value (μg L^{-1})		SERS			ICP-MS		
		Obtained Value (μg L^{-1})	Recovery (%)	RSD (%, n = 3)	Obtained Value (μg L^{-1})	Recovery (%)	RSD (%, n = 3)
Lake water	3	3.1718	105.73	1.40	2.9584	98.61	0.36
	6	5.9238	98.73	5.10	5.9064	98.44	1.37
	7	6.8717	98.17	4.42	6.9794	99.71	0.15
Tap water	2	2.1053	105.27	2.70	2.0133	100.67	0.70
	5	4.9294	98.59	5.59	4.9425	98.85	0.94
	8	8.1370	101.71	5.57	8.0840	101.05	0.03

Reference

1. H. Yuan, C.G. Khoury, H. Hwang, C.M. Wilson, G.A. Grant, T. Vo-Dinh, Nat. Nanotechnol., 2012, **23**, 075102.
2. S. Atta, T. Vo-Dinh, Analyst, 2023, **148**, 1786-1796.
3. S. Tanwar, V. Kaur, G. Kaur, T. Sen, J. Phys. Chem. Lett. 2021, **12**, 8141-8150.
4. S. Tanwar, K.K. Haldar, T. Sen, J. Am. Chem. Soc, 2017, **139**, 17639-17648.
5. S.S. Li, Q.Y. Guan, M.M. Zheng, Y.Q. Wang, D.J. Ye, B. Kang, J.J. Xu, H.Y. Chen, Chem. Sci., **2017**, 8, 7582-7587.
6. A.M. Fales, H. Yuan, T. Vo-Dinh, J. Phys. Chem. C, 2014, **118**, 3708-3715.
7. L. Li, W.S. Chin, ACS Appl. Mater, 2020, **12**, 37538-37548.
8. T.A. Saleh, M.M. Al-Shalalfeh, A.A. Al-Saadi, Mater Res Bull, 2017, **91**, 173-178.
9. H. Fang, X. Zhang, S.J. Zhang, L. Liu, Y.M. Zhao, H.J. Xu, Sens. Actuators B Chem., 2015, **213**, 452-456.
10. Y. Zhang, J. Liu, X. Wu, W. Tao, Z. Li, Anal. Chim. Acta, 2020, **1131**, 68-79.
11. Z. Ma, Y. Ma, M. Gu, X. Huo, S. Ma, Y. Lu, Y. Ning, X. Zhang, B. Tian, Z. Feng, Nanomaterials, 2020, **10**, 1924.
12. X. Gong, Y. Liu, Z. Yang, S. Shuang, Z. Zhang, C. Dong, Anal. Chim. Acta, 2017, **968**, 85-96.
13. S. Ghayyem, A. Swaidan, A. Barras, M. Dolci, F. Faridbod, S. Szunerits, R. Boukherroub, Talanta, 2021, **226**, 122082.
14. S. Bhatt, G. Vyas, P. Paul, ACS Omega, 2022, **7**, 1318-1328.
15. J. Valdez, I. Gómez, One-step green synthesis of metallic nanoparticles using sodium alginate, J. Nanomater., 2016, **2016**, 9790345.
16. B. Lv, Z. Sun, J. Zhang, C. Jing, Colloids Surface A, 2017, **513**, 234-240.
17. X.Y. Wang, H. Cheng, Y.Z. Min, X. Li, L.J. You, J.M. Li, Compos Part B-eng, 2022, **239**, 109959.